Fabrication of an ultra-nanocrystalline diamond-coated silicon wire array with enhanced field-emission performance

Fabrication of an ultra-nanocrystalline diamond-coated silicon wire array with enhanced field-emission performance

Yu-Fen Tzeng[1]**, Kao-Hsiang Liu**[2]**, Yen-Chih Lee**[1]**, Sue-Jian Lin**[1]**, I-Nan Lin**[3]**, Chi-Young Lee**[4] **and Hsin-Tien Chiu**[2]

[1] Department of Materials Science and Engineering, National Tsing Hua University, Hsinchu 30043, Taiwan, Republic of China
[2] Department of Applied Chemistry, National Chiao Tung University, Hsinchu 30050, Taiwan, Republic of China
[3] Department of Physics, Tamkang University, Tamsui 251, Taiwan, Republic of China
[4] Center of Nanotechnology, Materials Science and Microsystems, National Tsing Hua University, Hsinchu 30043, Taiwan, Republic of China

E-mail: cylee@mx.nthu.edu.tw and htchiu@cc.nctu.edu.tw

Abstract

Large-area ultra-nanocrystalline diamond-coated silicon nanowire (UNCD/SiNW) field-emitter arrays were prepared by the deposition of ultra-nanocrystalline diamond (UNCD) on the tips of arrays of silicon nanowires (SiNWs) with uniform diameters. The electron field-emission (EFE) behavior of UNCD/SiNW arrays as well as that of the SiNW arrays has been observed. The SiNWs exhibit good electron field-emission properties with turn-on fields (E_0) of about 7.6 V μm^{-1}, which is superior to the EFE properties of planar-silicon materials. The turn-on fields are related to the diameter of the SiNWs. Coating the SiNWs with a UNCD film further improves their EFE properties. The threshold field for attaining $J_e = 0.1$ mA cm^{-2} EFE current density is 16.0 V μm^{-1} for bare SiNWs and 10.2 V μm^{-1} for UNCD/SiNWs. The improvement in EFE properties due to the UNCD coating is presumably due to the lower work function of field emission of the UNCD materials, compared to that of the silicon materials.

1. Introduction

In the past decade one-dimensional nanomaterials, such as nanotubes and nanowires, have been extensively studied. They have received increasing attention because of their novel physical properties and their potential applications as devices [1–3]. Diamond films have attracted considerable scientific interest as EFE materials [4, 5]. Moreover, diamonds in microtip geometry [6–9] have been shown to reduce the turn-on field and achieve large EFE current densities, comparable to those of carbon nanotubes (CNTs) [10–15]. In the present work, we combined the superior properties of UNCD with an array of SiNWs to enhance the electron field-emission behavior. The UNCD/SiNW field emitters were prepared by microwave plasma-enhanced chemical vapor deposition (MPECVD) of UNCD on SiNW arrays with tunable diameters. The preparation procedure is shown in scheme 1. The SiNW arrays were prepared by a galvanic displacement [16] reaction in a HF/AgNO$_3$ solution using silicon wafers that were uniformly coated with gold particles. A thin layer of UNCD was coated on the resulting SiNWs using MPECVD, producing UNCD/SiNW field-emitter arrays.

2. Experimental details

n-type Si(100) substrates were cut into 1.0×1.0 cm^2 squares and cleaned using the standard RCA process. The silicon wafers were coated with gold by sputtering for 1, 2, 5 and 10 s; extended sputtering times led to thicker layers of gold, allowing for the formation of larger grains of gold on the
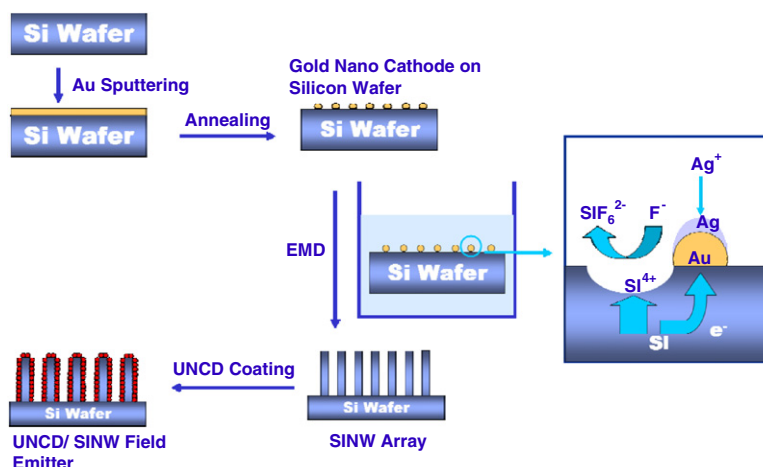
Scheme 1. The preparation procedure of the UNCD/SiNW field emitters.
(This figure is in colour only in the electronic version)

silicon wafer. The gold-deposited silicon substrates were then heated under an argon atmosphere at 1073 K for 3 h to form gold particles on the silicon wafer.

The gold nanoparticle-coated silicon wafer fragments were immersed in an aqueous solution of 0.103 M $AgNO_3$ in 12 ml of 48% HF for 30 min. The wafers were removed from the solution and washed with concentrated HNO_3 and deionized water to remove the coated silver and gold and any unreacted reagents, followed by drying with a stream of nitrogen.

Diamond films were grown on the prepared SiNW arrays by the microwave plasma-enhanced chemical vapor deposition process (MPECVD) using an ASTex 5400 reactor. CH_4/H_2 gases with a flow rate of 1 sccm/99 sccm were excited by 600 W microwaves, while the total pressure in the chamber was maintained at 120 Torr. The SiNW-array substrates were maintained at around 673 K during the growth of the diamond films.

The films were characterized using Raman spectroscopy (Renishaw, 632.8 nm), scanning electron microscopy (SEM: JEOL JSM-6500F at 15 kV), energy-dispersive x-ray (EDX) analysis (Oxford Link Pentafet) and transmission electron microscopy (TEM: JEOL JEM-2010F at 200 kV and JEOL JEM-4000EX). The EFE properties of the diamond-coated SiNWs were measured with a tunable parallel plate set-up, in which the sample-to-anode distance was varied using a micrometer. The current–voltage (I–V) characteristics were measured using an electrometer (Keithley 237) under pressures below 10^{-6} Torr. The EFE parameters were extracted from the obtained I–V curves by using the Fowler–Nordheim model. The maximum available voltage of the set-up is 1100 V, and the current was restricted to 10 mA.

3. Results and discussion

According to Zhu's studies, SiNW arrays can be prepared by immersing a silicon wafer into an aqueous solution of $AgNO_3$ and HF in an electroless metal deposition (EMD) process [16–22]. The Ag nanoparticles, produced from the reduction of the Ag^+ deposit on the silicon wafer surface, serve

as the cathode while the surroundings act as the anode. This essentially produces a nanosized electrochemical cell array, resulting in the formation of SiNWs. The drawback of this process was that the Ag clusters easily aggregated, forming large Ag particles of various sizes, which in turn resulted in silicon wires with a large size distribution. To improve the uniformity of the SiNW arrays, gold nanoparticles were used as the cathode instead, followed by the same EMD process. In summary, the SiNW arrays were prepared by a galvanic displacement reaction of a silicon wafer coated with uniform gold particles in a HF/$AgNO_3$ solution.

Figures 1(a)–(c) show scanning electron microscopy (SEM) images of the as-prepared SiNW arrays for different gold sputtering periods. SiNWs with uniform diameters and lengths of up to 50 μm were observed. The energy dispersive x-ray (EDX) spectrum suggests that the only element present is Si. Figure 1(d) shows a transmission electron microscopy (TEM) image of an individual SiNW obtained from the SiNW array; the diameter of the wire was about 25 nm, which is approximately the diameter of the gold particles coated on the silicon wafer. The inset of figure 1(d) is a high-resolution TEM (HRTEM) image of this wire indicating that the wire direction is [100].

In order to study in detail the relationship between the particle size of the gold coating on the silicon wafer and the diameter of the SiNWs obtained, the gold sputtering period was varied. Figure 2 shows that the average diameter of the SiNWs is proportional to the size of the gold particles, which in turn is proportional to the sputtering period. There is a direct correlation between the particle sizes of the gold coating and the diameters of the SiNWs. Shorter sputter times resulted in thinner SiNWs, since they produced a thinner gold film and therefore smaller particles of gold after heating. Thicker gold films produced from lengthy sputter times formed larger particles after heating, leading to thicker SiNWs. Particle sizes and therefore the diameters of the SiNWs were controlled through careful modulation of the gold sputtering time. SiNW arrays with average wire diameters of 20 and 35 nm, obtained by etching of 12 and 20 nm gold-particle-coated silicon wafers, are shown in figures 1(b) and (c), respectively.
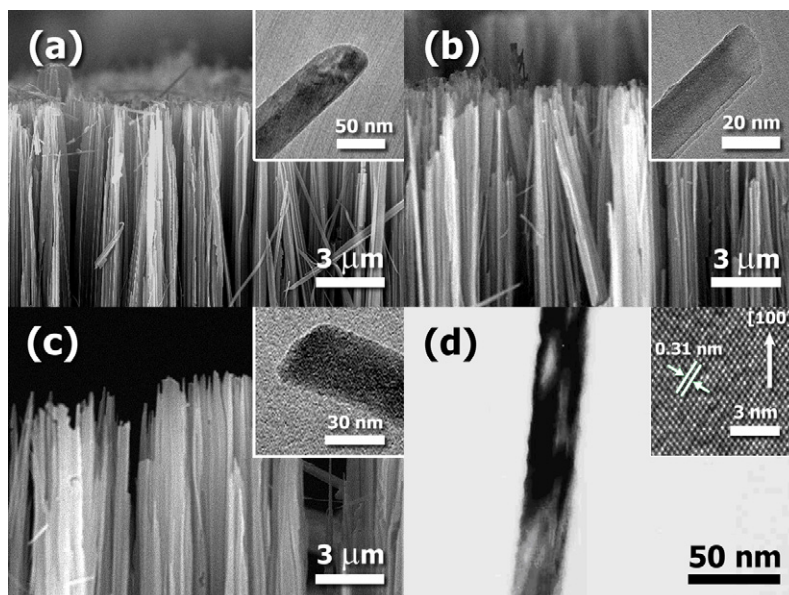
Figure 1. SEM images of the SiNW arrays, prepared by the galvanic displacement reaction of a gold-particle-coated silicon wafer in a HF/AgNO$_3$ solution. The gold sputtering periods are (a) 0 s, (b) 1 s and (c) 10 s. (d) The TEM and HRTEM images of an individual SiNW.
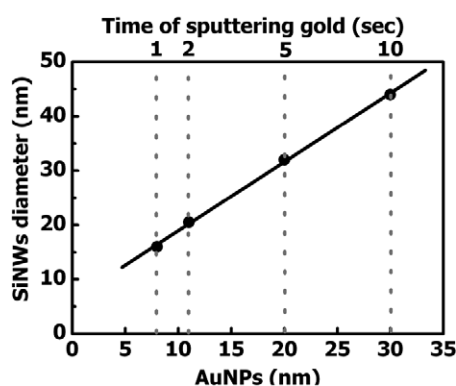

Figure 2. Variation of the grain size of gold nanoparticles on the silicon wafer and the diameter of the SiNWs that were obtained with varying gold sputtering times.
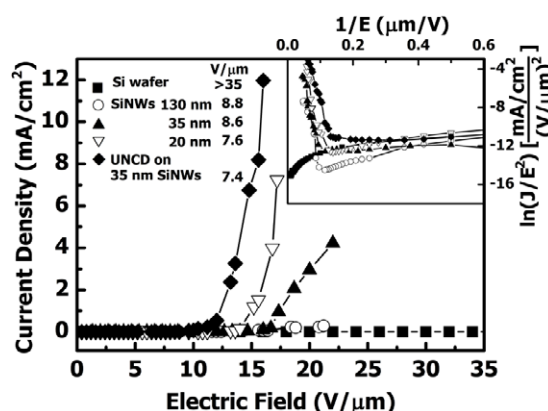

Figure 3. EFE properties of silicon wafer, SiNW arrays with various wire diameters, and UNCD/SiNW arrays.

Figure 3 illustrates that the SiNWs exhibit very good EFE properties even though the silicon wafer is essentially non-emitting. The EFE current density (J_e) increases as the diameters of the SiNWs decrease. At an applied field of 22.0 V μm^{-1}, $(J_e)_A = 0.3$ mA cm^{-2} for the 130 nm SiNWs (type A, open circles) and $(J_e)_B = 4.2$ mA cm^{-2} for the 35 nm SiNWs (type B, solid triangles), whereas the $(J_e)_C$ is larger than 40 mA cm^{-2} for the 20 nm SiNWs (type C, open triangles), which is out of range of the measuring apparatus. The threshold field (E_t) required to reach a emission current density of $(J_e)^o = 0.1$ mA cm^{-2} decreases as the diameter of the SiNWs decreases. $(E_t)_A = 17.0$ V μm^{-1} for the 130 nm SiNWs (open circles), $(E_t)_B = 16.0$ V μm^{-1} for the 35 nm SiNWs (solid triangles) and $(E_t)_C = 14.0$ V μm^{-1} for the 20 nm SiNWs (open triangles). These results are summarized in table 1(a), indicating clearly the improvements of EFE properties attained by decreasing the size of the SiNWs. To deduce the intrinsic electron field-emission parameters for

these SiNWs, the normalized electron field-emission current density (ln J/E^2) of the SiNWs was plotted against the inverse of the applied field ($1/E$) to give a Fowler–Nordheim (F–N) plot [23, 24]. The F–N plots for the SiNWs are shown in the inset of figure 3, illustrating that the turn-on field (E_o), which is defined as the intersection of two straight lines corresponding to the slope of the low-field and high-field segments of the F–N plots, decreases steadily with the size of the SiNWs. The effective work function $\Phi_e = \Phi^{3/2}/\beta$, which is defined as the ratio of the work function (Φ) and field-enhancement factor (β), decreases steadily with the size of the SiNWs. These intrinsic EFE parameters are summarized in table 1(b), which clearly shows that the improvements on EFE gained by small SiNWs is due to the increase in the field-enhancement factor (β), as the work functions of the SiNWs are the same ($\Phi_{Si} = 4.1$ eV) [25, 26].

To further improve the electron field-emission properties of SiNWs, a thin layer of UNCD was coated on an array
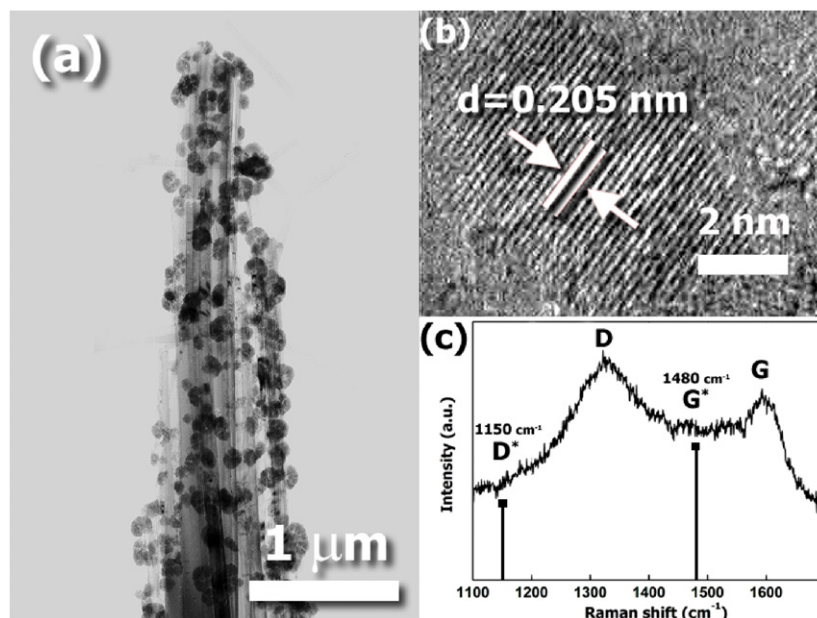
Figure 4. (a) The TEM image of a UNCD/SiNW bundle, (b) HRTEM of an individual diamond particle, (c) Raman spectrum of the UNCD/SiNWs.

Table 1. The electron field-emission properties of SiNWs of various diameters and UNCD/SiNWs.

		Si(100)	SiNW(A)	SiNW(B)	SiNW(C)	UNCD/SiNW
(a)	Average wire diameter (nm)	—	130	35	20	40–50
	J_e (mA cm^{-2})[a]	—	∼0.3	4.2	>40	>40
	J_e (mA cm^{-2})[b]	—	∼0.1	∼0.1	∼1.2	>7.0
	E_t (V μm^{-1})[c]	—	17.0	16.0	14.0	10.2
(b)	E_o (V μm^{-1})	>35	8.8	8.6	7.6	7.4
	Φ_e (eV)	4.1 [25, 26]	0.022	0.0203	0.020	0.016

[a] The electron field-emission current density measured at 22.0 V μm^{-1} applied field.

[b] The electron field-emission current density achieved at 15.0 V μm^{-1} applied field.

[c] The electric field necessary for attaining $J_e = 0.1$ mA cm^{-2}.

of 35 nm SiNWs using the MPECVD process. Figure 4(a) shows the TEM image of an UNCD/SiNW bundle. The TEM micrograph reveals that the SiNWs are coated with a uniform diamond agglomerate, which consists of aggregates of nanosized diamond particles. The HRTEM image of an individual diamond particle is shown in figure 4(b), indicating that the lattice spacing of the fringes is about 0.205 nm, which is a typical lattice parameter for diamond. Moreover, this figure shows that the grains of UNCD are about ∼7 nm in size. The Raman spectra shown in figure 4(c) indicate that these UNCD/SiNWs contain a D*-band at ∼1150 cm^{-1}, a D-band at 1350 cm^{-1}, a G*-band at ∼1480 cm^{-1} and a G-band at 1580 cm^{-1}, typical Raman spectra for UNCD [27].

The UNCD coating markedly improves the EFE properties of the SiNWs. Figure 3 and inset (solid rhombus) reveal that the electron field emission of UNCE/SiNWs can be turned on at much lower electric fields ((E_o)$_{UNCD}$ = 7.4 V μm^{-1}, table 1(b)), attaining markedly larger emission current densities over the measurable range (i.e. >40.0 mA cm^{-2} at an applied field of 22.0 V μm^{-1}). Table 1(a) indicates that $E_t = 10.2$ V μm^{-1} for UNCD/SiNWs, which is markedly smaller than the E_t for bare SiNWs. Moreover, the EFE current densities corresponding to an applied field of 15 V μm^{-1}

are about 0.1 mA cm^{-2} for bare SiNWs and larger than 7.0 mA cm^{-2} for UNCD/SiNWs. These results illustrate clearly the beneficial effect of the UNCD coating on the EFE current density of SiNWs.

The effective work functions of these nanowires were estimated from the high-field region of the slope of the F–N plots and are listed in table 1(b). This table indicates that the value of the effective work function of UNCD/SiNWs is much smaller than that of the bare SiNWs. The true value of the work function of these materials cannot be unambiguously estimated due to the complicated geometry of the nanowires. Nevertheless, these results strongly imply that UNCD possesses a pronouncedly smaller work function than the silicon materials. Since both nanowires are of similar geometry, i.e. they have a very high aspect ratio but are closely packed, the field-enhancement factor (β) of UNCD/SiNWs is not expected to differ very much from that of SiNWs. The UNCD/SiNWs are likely to have a slightly smaller β-factor due to slightly larger diameters, but the difference is expected to be small. Therefore, the main factor resulting in a smaller Φ_e for UNCD/SiNWs is presumably the smaller true work function of UNCD (Φ_{UNCD}), compared to the true work function of silicon (Φ_{Si}).

It should be noted that although the turn-on field (E_0) for EFE of UNCD/SiNW is considerably larger than that for CNTs, the emission current density for these UNCD/SiNWs is large enough (>7 mA cm^{-2} at 15 V μm^{-1}) for practical applications as electron field emitters. Moreover, the stability of EFE properties of UNCD/SiNWs is considerably better than that of CNTs, not to mention SiNWs. The SiNW fabrication procedure is a self-aligning and electroless process, which is easily scalable, as is the MPECVD process for coating UNCD films. The processing stability for synthesizing UNCD/SiNWs is greatly increased compared to growing CNTs. Taking all these factors into consideration, the UNCD/SiNWs are superior to CNTs for electron emitter applications.

4. Conclusion

In summary, SiNW arrays, which possess superior electron field-emission properties compared to planar-silicon materials, were fabricated from Si(100) substrates by a galvanic etching process. Coating the SiNWs with a thin layer of UNCD film further improves the electron field-emission properties of these materials. The threshold field for attaining $J_e = 0.1$ mA cm^{-2} EFE current density decreases from 16.0 V μm^{-1} for bare SiNWs to 10.2 V μm^{-1} for UNCD/SiNWs, whereas the EFE current density at 15 V μm^{-1} applied field increases from about 0.1 mA cm^{-2} for the bare SiNWs to greater than 7.0 mA cm^{-2} for the UNCD/SiNWs. The effective work function for field emission is 0.0203 and 0.0160 eV for bare SiNWs and UNCD/SiNWs, respectively. The lower work function of field emission of the UNCD materials, compared with that of the silicon materials, is presumed to be the main factor in improving the electron field-emission properties of the materials.

Acknowledgments

References

[1] Liber C M 2001 *Sci. Am.* **285** 58
[2] Li D, Wu Y, Fan R, Yang P and Majumdar A 2003 *Appl. Phys. Lett.* **83** 3186
[3] Li D, Wu Y, Kim P, Shi L, Yang P and Majumdar A 2003 *Appl. Phys. Lett.* **83** 2934
[4] Wang C, Garcia A, Ingram D C, Lake M and Kordesch M E 1991 *Electron. Lett.* **27** 1459
[5] Geis M W, Efremow N, Woodhouse J, Mcalese M, Marchywka M, Socker D and Hochedez J 1991 *IEEE Electron Devices Lett.* **12** 456
[6] Sotgiu G and Schirone L 2005 *Appl. Surf. Sci.* **240** 424
[7] Djubua B C and Chubun N N 1991 *IEEE Trans. Electron Devices* **38** 2314
[8] Givargizov E I, Zhirnov V V, Stepanova A N, Rakova E V, Kieselev A N and Plekhanov P S 1995 *Appl. Surf. Sci.* **87/88** 24
[9] Krauss R *et al* 2001 *J. Appl. Phys.* **89** 2958
[10] Dean K A and Chalamala B R 2000 *Appl. Phys. Lett.* **76** 375
[11] Zhu W, Bower C, Zhou O, Kochanski G and Jin S 1999 *Appl. Phys. Lett.* **75** 873
[12] Jiang K, Li Q and Fan S 2002 *Nature* **419** 801
[13] Bonard J M, Stockli T, Noury O and Chatelain A 2001 *Appl. Phys. Lett.* **78** 2775
[14] Murakami H, Hirakawa M, Tanaka C and Yamakawa H 2000 *Appl. Phys. Lett.* **76** 1776
[15] Xu Z, Bai X D, Wang E G and Wang Z L 2005 *Appl. Phys. Lett.* **87** 163106
[16] Kuznetsov G V, Skryshevsky V A, Vdovenkova T A, Tsyganova A I, Gorostiza P and Sanz F G 2001 *J. Electrochem. Soc.* **148** C528
[17] Peng K-Q, Yang Y-J, Gao S-P and Zhu J 2002 *Adv. Mater.* **14** 1164
[18] Peng K-Q, Yang Y-J, Gao S-P and Zhu J 2003 *Adv. Funct. Mater.* **13** 127
[19] Peng K-Q and Zhu J 2003 *J. Electrochem. Soc.* **558** 35
[20] Peng K-Q, Huang Z-P and Zhu J 2004 *Adv. Mater.* **16** 73
[21] Peng K-Q, Wu Y, Fang H, Zhong X-Y, Xu Y and Zhu J 2005 *Angew. Chem.* **117** 2797
[22] Peng K, Hu J, Yan Y, Wu Y, Fang H, Xu Y, Lee S-T and Zhu J 2006 *Adv. Funct. Mater.* **16** 387
[23] Fowler R H and Nordheim L W 1928 *Proc. R. Soc.* A **119** 173
[24] Nordheim L 1928 *Proc. R. Soc.* A **121** 626
[25] Ding M, Kim H and Akinwande A I 1999 *Appl. Phys. Lett.* **75** 823
[26] Zorba V, Tzanetakis P and Fotakis D G 2006 *Appl. Phys. Lett.* **88** 081103
[27] Ferrari C and Robertson J 2001 *Phys. Rev.* B **63** 121405(R)